V European Conference on Computational Fluid Dynamics
ECCOMAS CFD 2010
J. C. F. Pereira and A. Sequeira (Eds)
Lisbon, Portugal, 14–17 June 2010

RANS BASED NUMERICAL STUDY OF HYDROGEN MILD COMBUSTION

E. Mollica[*], E. Giacomazzi[†], and A. Di Marco[††]

[*] SPAL Automotive s. r. l.
Via per Carpi 26, 42015 Correggio Italy
e-mail: e.mollica@spal.it

[†] ENEA Casaccia, ENE-IMP
Via Anguillarese 301, 00123 S.M. Galeria Rome Italy
e-mail: eugenio.giacomazzi@enea.it

[††] University Roma TRE, Industrial and Mechanical Engineering Department
Via della Vasca Navale 74, 00146 Rome Italy
e-mail: adimarco@uniroma3.it

Key words: Hydrogen, flameless combustion, computational fluid dynamics.

Abstract. *In this article a combustor burning hydrogen and air in MILD regime is numerically simulated by means of RANS technique. The purpose is to analyse the influence of main parameters such as dilution, preheating, internal recirculation and radiation. All the results of the simulations show a good agreement with experimental data. The flow configuration is characterized by strong exhaust gas recirculation with high air preheating temperature. As a consequence, the reaction zone is characteristically broad and the temperature and concentrations fields are found to be sufficiently homogeneous and uniform, leading to a strong abatement of nitric oxide emissions. It is observed that the reduction of thermal gradients is achieved mainly through the extension of combustion in the whole volume of the combustion chamber, so that a flame front no longer exists ("flameless oxidation"). Belonging of present MILD regime to the volumetric region of the Borghi's diagram is checked, as well as the fulfilment of Oberlack and Peters' criterion. Effects of preheating, further dilution provided by inner recirculation, effects of radiation and wall temperature for the present hydrogen/air MILD combustor are finally analysed.*

1 INTRODUCTION

During the past decade and especially in these very last years the abatement of emissions of pollutants has been representing a relevant topic of research. Special emphasis has been particularly given to those novel combustion regimes which have the intrinsic potential to lessen pollution.

MILD oxidation is a promising combustion technique for the reduction of pollutant emissions, which is achieved by lowering the temperature increase in the process [1– 7]. Its main principle of operation lies on massive exhaust gas recirculation, so that the temperature increase of reactants and the oxygen concentration can be strongly reduced [8–13]. Such a technique, relying on a good control of thermal peaks (*i.e.*, homogeneous thermal field), leads to an abrupt abatement of emissions than traditional processes.

It has been held that preheating of combustion air causes significant increase in nitric oxide emissions, due to high temperatures [1,2,5,9,13]. However, in circumstances of low oxygen concentration it is possible to observe a substantial suppression of pollutant emissions [1,2,5,8,11]. Nevertheless, in presence of such high dilution levels, combustion can take place in stable way only as long as the mixture is preheated higher than the auto–ignition temperature [1,5,7,14].

Hence, it is possible to introduce the following definition for the MILD combustion regime [1]: "A combustion process is named MILD when the inlet temperature of the reactant mixture is higher than mixture auto–ignition temperature whereas the maximum allowable temperature increase with respect to inlet temperature during combustion is lower than mixture auto–ignition temperature (in Kelvin)".

The gap existing between the apparently contrasting goals of minimization of pollutant emissions and improvement of process efficiency (regenerative and recuperative burners) can be potentially lowered in MILD combustion because of the high levels of dilution characteristic of the mixture (*i.e.*, low oxygen concentrations) leading to a strong reduction of temperature peaks in the combustion chamber.

In MILD regime reactions occur at lower rates (higher characteristic combustion times) than in traditional processes, so that the characteristic times of chemical kinetics and fluid–dynamics are almost of the same order of magnitude and the Damkohler number is very close to unity [10,15]. The combustion zone is no longer concentrated close to the flame front but is extended over the whole combustion chamber, resulting in complete disappearance of any luminous emission: hence the name "flameless combustion" [3,4,12,13,16]. Moreover, it can be noticed that this volumetric distributed combustion approaches the mixing conditions of a WSR [1,7,10,12,15,16].

The enlargement of the combustion region, as said before, is principally obtained by providing high internal recycle levels [12,13,16]. Wunning [13] showed that as long as the reacting mixture temperature is high a stable combustion regime can be obtained for high recirculation factors.

The mathematical condition beyond which MILD combustion can be established was first rigorously obtained by Oberlack and Peters [15]. In particular, studying the case of a Well Stirred Reactor in adiabatic conditions with chemical kinetics described by a simple one–step Arrhenius mechanism, they derived MILD mathematical condition

$$\frac{E/\mathrm{R}}{T_{\mathrm{inl}}} < 4\left(1+\frac{c_{\mathrm{P}}\,W_{\mathrm{f}}\,T_{\mathrm{inl}}}{\Delta H\;Y_{\mathrm{f}}}\right) \tag{1}$$

where Y_f and W_f are the fuel mass fraction and molecular weight, ΔH is the enthalpic increment, c_p is the specific heat, T_{inl} is the inlet temperature, E is the global reaction activation energy and R is the universal gas constant. Condition expressed by eq. (1)

was found by observing that in MILD combustion ignition and extinction phenomena are suppressed. This means that the curve T versus Damkohler number Da (see fig. 1) does not show the S–shape typical behaviour of classical combustion processes. As a matter of fact temperature depends monotonically on Da and the branching points I and Q (corresponding to ignition and extinction, respectively) no longer exist.

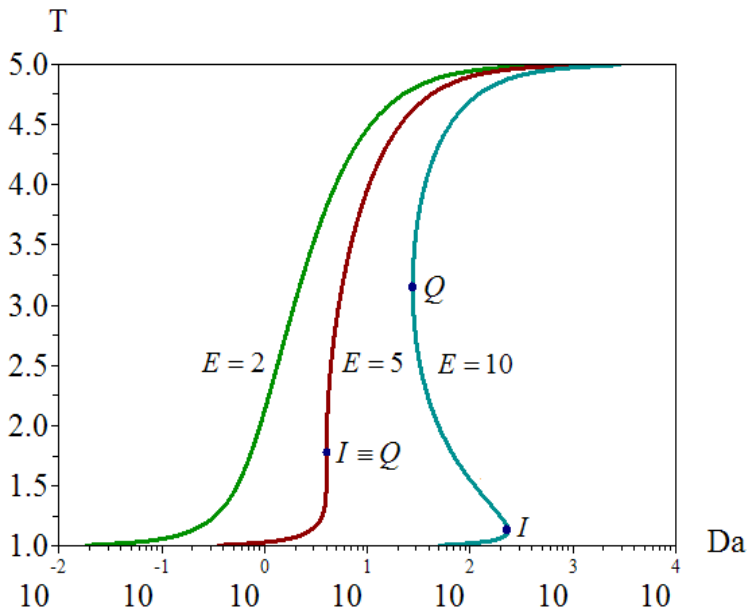

Figure 1: Dependence of steady state burner temperature on the Damkohler number for $\Delta H\ Y_{\mathrm{f}}\ c_{\mathrm{P}}^{-1}\ W_{\mathrm{f}}^{-1}\ T_{\mathrm{inl}}^{-1} = 4$ [15].

It is observed that eq. (1) can be approximated as [1, 12]

$$\frac{\Delta H_{\mathrm{R}}\ Y_{\mathrm{f}}}{c_{\mathrm{P}}\ W_{\mathrm{f}}\ T_{\mathrm{inl}}} \approx \frac{T_{\mathrm{b}} - T_{\mathrm{inl}}}{T_{\mathrm{inl}}} \tag{2}$$

This identifies MILD combustion in terms of the burning temperature T_b and of the inlet preheating temperature T_{inl}. This criterion can also be written as

$$\vartheta \cdot \mathrm{Ze} \leq 4 \tag{3}$$

introducing the temperature ratio

$$\vartheta = \frac{T_{\mathrm{b}}}{T_{\mathrm{inl}}} \tag{4}$$

and the Zeldovich number

$$\mathrm{Ze} = \frac{T_{\mathrm{a}}}{T_{\mathrm{b}}} \cdot \frac{T_{\mathrm{b}} - T_{\mathrm{inl}}}{T_{\mathrm{b}}} = \frac{T_{\mathrm{a}}}{T_{\mathrm{b}}} \cdot \frac{\vartheta - 1}{\vartheta} \tag{5}$$

where T_a is the activation temperature.

In the present article MILD combustion of hydrogen and air experimentally studied by Derudi *et al.* [8,10,11,17] is numerically simulated. Section 2 describes the experimental apparatus and the numerical model used in this study. In section 3 numerical results are reported and compared with experimental data. A theoretical interpretation of hydrogen MILD combustion is finally proposed.

2 COMBUSTION BURNER AND NUMERICAL MODEL

In the present paper Derudi's [8,10,11,17] laboratory–scale burner for MILD combustion has been numerically reproduced in the case of pure hydrogen as a fuel. The experimental apparatus, shown in fig. 2, is characterized by high internal recirculation (achieved by a proper aerodynamic design of the combustion chamber). An external recycle of burned gases is simulated vitiating the air and the fuel with a certain amount of nitrogen. The burner can be divided in two sections, a lower one, attaining the air preheating zone (shown in fig. 2, D) and an upper one, where the combustion chamber is located (fig. 2, A). Both sections are enclosed with refractory insulation (fig. 2, H, G).

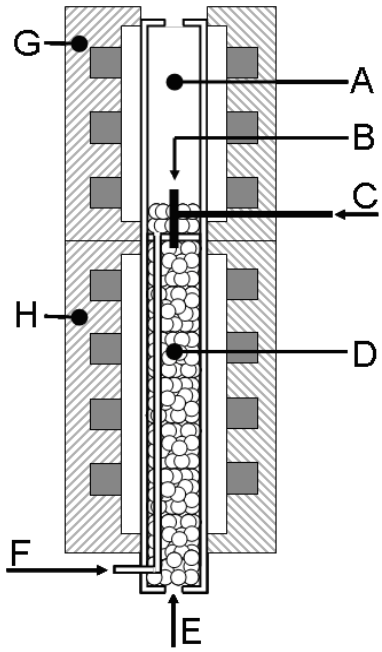

Figure 2: Sketch of the laboratory-scale MILD burner used by Derudi et al. [8,10,11,17].

The top of the combustor has a small central hole and three larger ones eccentrically located, so that the combustor has a rotational symmetry of 120°.

As described in detail by Cavigiolo [8] and Galbiati [11] the air flux vitiated with nitrogen enters the preheating zone (fig. 2, E, D), heats up and flows through the inlet of a high velocity nozzle 80 mm long (fig. 2, B); the fuel is injected perpendicularly (fig. 2, C) into the nozzle via a capillary pipe (1mm internal diameter). Before the reactants reach the combustion chamber a partial premix of fuel and air streams occurs in the nozzle but no reaction takes place because of the short residence time.

Temperature measurements were obtained by three thermocouples located at 100 mm, 170 mm and 300 mm above the nozzle outlet (the first one was 10 mm shifted from the centre). NO concentration at the burner exit was carried out via a gas analyzer.

Since the numerical simulations of the present paper aim to reproduce a slice of 120° of the combustion chamber only it is necessary to calculate the flux properties at the outlet of the nozzle (*i.e.*, entering the combustion chamber). This can be done using a one–dimensional model, where the hypotheses of ideal, steady, adiabatic, non viscous flow are considered:

$$\dot{m}_3 = \dot{m}_1 + \dot{m}_2 \tag{6}$$

$$\dot{m}_1 u_1 + p_1 A_1 + \dot{m}_2 u_2 + p_2 A_2 = \dot{m}_3 u_3 + p_3 A_3 \tag{7}$$

$$\dot{m}_3 c_{P_3} T_3 = \dot{m}_1 c_{P_1} T + \dot{m}_2 c_{P_2} T_2 \tag{8}$$

$$\begin{cases} \dot{m}_3 Y_{3,H_2} = \dot{m}_2 Y_{2,H_2} \\ \dot{m}_3 Y_{3,O_2} = \dot{m}_1 Y_{1,O_2} \\ \dot{m}_3 Y_{3,N_2} = \dot{m}_1 Y_{1,N_2} + \dot{m}_2 Y_{2,N_2} \end{cases} \tag{9}$$

$$p_i = \rho_i \, R \, T_i \left(\frac{Y_{i,H_2}}{W_{H_2}} + \frac{Y_{i,O_2}}{W_{O_2}} + \frac{Y_{i,N_2}}{W_{N_2}} \right) \tag{10}$$

is the universal gas constant, A_i is the area, u_i is the velocity, Y_{iH} is the hydrogen mass fraction and W_H the hydrogen molecular weight. The air flux is represented by $i=1$, the fuel flux is denoted by $i=2$ and the mixture entering into the combustion chamber (nozzle outlet) by $i=3$.

In fig. 3 the temperature at the outlet of the nozzle (*i.e.*, at the combustion chamber inlet) as a function of preheating temperature is shown. The solid line is relative to the analytical model of eqs. (6) – (10). The dots are relative to numerical results of the mixing device obtained with 3D simulations, performed by Fluent 6.3, where Spalart–Allmaras [18] turbulence model was used. It can be observed a good agreement between the model and the results of the numerical simulations. The complete homogeneity of the mixture at the injection nozzle's outlet was checked and verified.

Since the preheating oven efficiency η is not precisely known, the error associated with this uncertainty can be estimated by a sensitivity analysis of the burner inlet temperature T_3 with η. It was observed that the maximum error associated with this preliminary calculation is about 4% for a preheating oven efficiency $\eta=0.9\text{-}0.95$ [19].

In this work five experimental conditions from Derudi [10] have been simulated. The preheating temperature, the upper oven temperature and the recirculation factor are reported in tab. 1. The internal recirculation factor is one of the most important parameters that strongly influences the performance of a MILD combustion burner and can be defined as [8,10,11,17].

$$K_V = \frac{\left(\dot{m}_{air} + \dot{m}_{fuel} + \dot{m}_{inert}\right) \cdot \zeta}{\dot{m}_{air} + \dot{m}_{fuel}} \tag{11}$$

where $\dot{m}_{air}$, $\dot{m}_{fuel}$ and $\dot{m}_{inert}$ are the air mass flow rate, the fuel mass flow rate and inert mass flow rate, respectively; $\zeta=5$ [8,10,11,17] is the maximum recycle factor due to aerodynamic configuration. The properties of the mixture entering the combustion chamber (*i.e.*, mass flux, temperature and composition) resulting from previous calculations with the analytical model are reported in tab. 2.

The numerical simulations were developed modelling a 120° angular section of the burner. Morse's [20] modified k-ε turbulence model ($C_{1\varepsilon}=1.6$), Eddy Dissipation Concept for chemistry–turbulence interaction [21] and P_1 radiation model [22] have been adopted. From the chemistry point of view, the Warnatz [23] detailed mechanism (including 37 reactions) was used. To take into account Zeldovich [24] thermal NO production and NO formation through NO_2 creation/destruction pathway [25,26] further 10 reactions have been considered.

Before performing all the simulations pertaining the experimental cases, the solution independence from the mesh (which is an unstructured hybrid tetrahedral/hexahedral one) was verified for the first case of tab. 1, using three different meshes: 230.000, 320.000 and 1.070.000 cells. As shown in fig. 4, using the 320.000 cells mesh the solution independence can be considered as sufficiently verified.

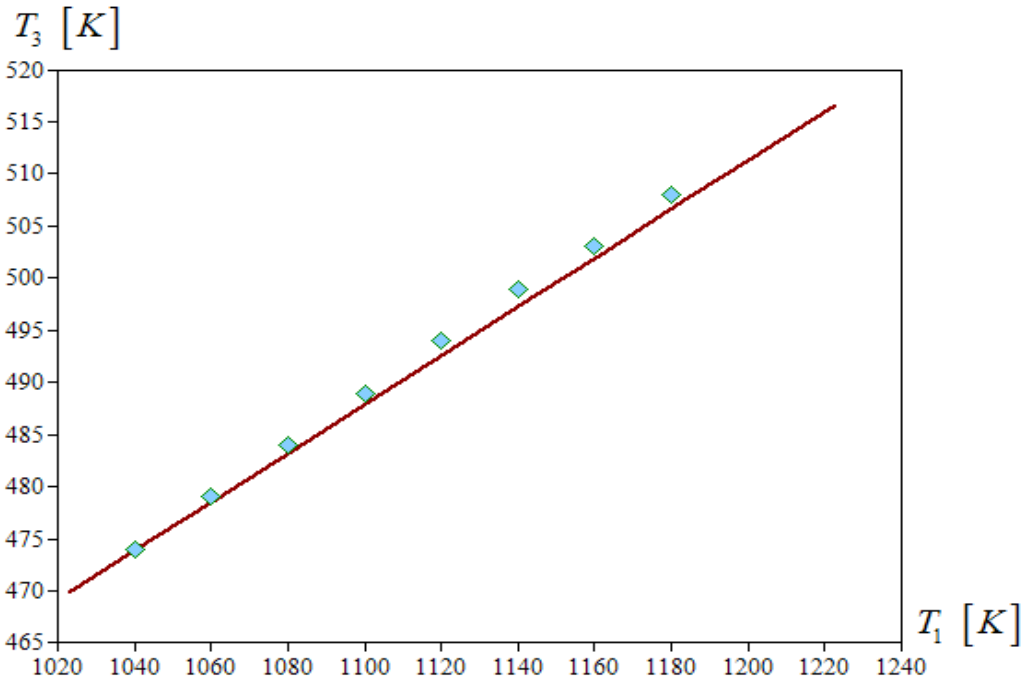

Figure 3: Burner inlet temperature as a function of air preheating temperature (solid line: analytical model; dots: numerical simulations).

Table 1: Preheating temperature, upper oven temperature and internal recycle factor for the five experimental conditions simulated in this work.

	$\hat{T}_1$ [°C]	T_{wall} [°C]	K_V
1	950	800	25.3
2	950	700	20.3
3	950	700	15.4
4	1100	700	13.0
5	1000	700	9.9

Table2: Mass flux, temperature, O_2 and H_2 mass fraction of the mixture entering into the combustion chamber (N_2 mass fraction is the complement to 1).

	$\dot{m}$ [kg/s]	T [K]	Y_{O_2}	Y_{H_2}
1	$6.44 \cdot 10^{-5}$	517	$3.09 \cdot 10^{-2}$	$3.77 \cdot 10^{-3}$
2	$4.93 \cdot 10^{-5}$	579	$4.04 \cdot 10^{-2}$	$4.93 \cdot 10^{-3}$
3	$3.42 \cdot 10^{-5}$	702	$5.82 \cdot 10^{-2}$	$7.11 \cdot 10^{-3}$
4	$2.67 \cdot 10^{-5}$	903	$7.47 \cdot 10^{-2}$	$9.12 \cdot 10^{-3}$
5	$1.72 \cdot 10^{-5}$	1151	$1.16 \cdot 10^{-1}$	$1.41 \cdot 10^{-2}$

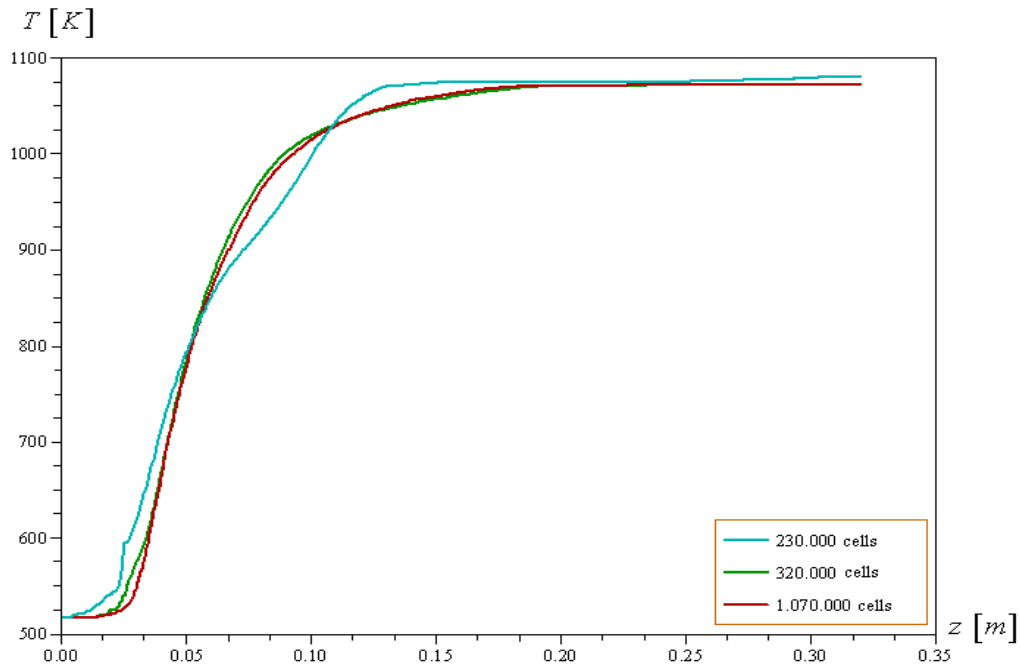

Figure 4: Grid independence analysis: temperature calculated at the burner centreline (first case of tab. 1).

3 RESULTS AND DISCUSSION

Figures 5 – 8 show the comparison between experimental data and numerical results, in terms of probes' temperatures and of NO emissions. As it can be observed the difference is about 4-5% and therefore it is of the same order of magnitude of the error by which the properties of the mixture entering into the chamber are affected. It is worth noting (see fig. 8) the capability of the numerical model to reproduce the levels of NO emission at the burner exit (few ppm, for high values of internal recirculation factor).

In fig. 9 streamlines coloured by temperature in a traversal plane inside the combustion chamber are shown, for the first case reported in tab. 1. The picture sheds light on the importance of recirculation (represented by the two main central vortices) by which the reactants are further heated prior to the combustion region. This is mainly achieved by means of heat transfer from burnt products, which are recirculated to mix with the incoming mixture. Moreover it can be noticed from fig. 9 that exhaust gases are entrained by the nozzle which operates as jet pump, so that the incoming stream with its high momentum is diluted by the recirculating burnt products: a new mixture exhaust gases, air, fuel and inert gases is then formed and heated up continuously.

The effect of further dilution of the mixture due to internally recirculated hot products results in additional preheating of reactants and in lowering oxygen concentration: these two features both affect the flame behaviour thus producing a volumetric combustion. Such a change of the flame structure yields to low Damkohler numbers (around unity), so that quite slow reactions take place.

From observation of figs. 9 – 11 it is possible to notice a widely distributed reaction region and no more a concentrated combustion as it happens in ordinary combustion processes [5]. In these operative conditions the heat release due to reactions is distributed, yielding to a considerably low temperature rise in the combustion chamber and, as a consequence, to an abrupt suppression of NO emissions. In contrast to traditional processes high gradients of temperature no longer occur (see figs. 12 – 15).

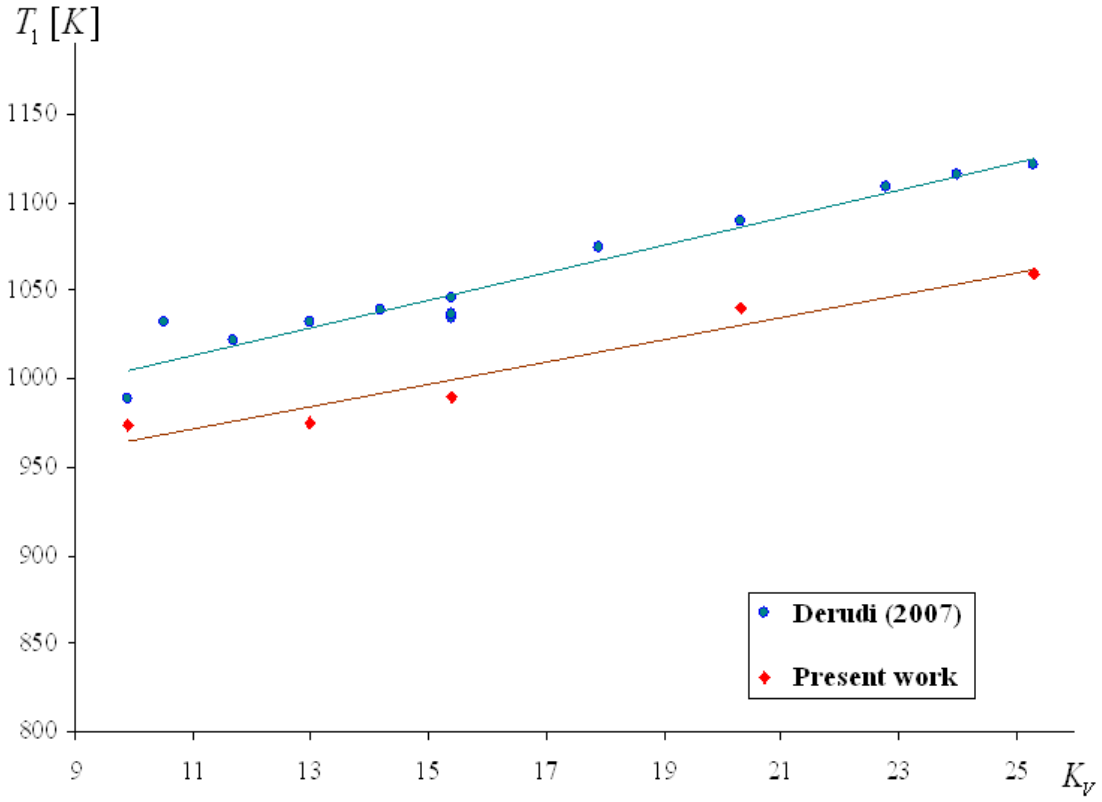

Figure 5: First probe temperature (z=0.3 m, r=0).

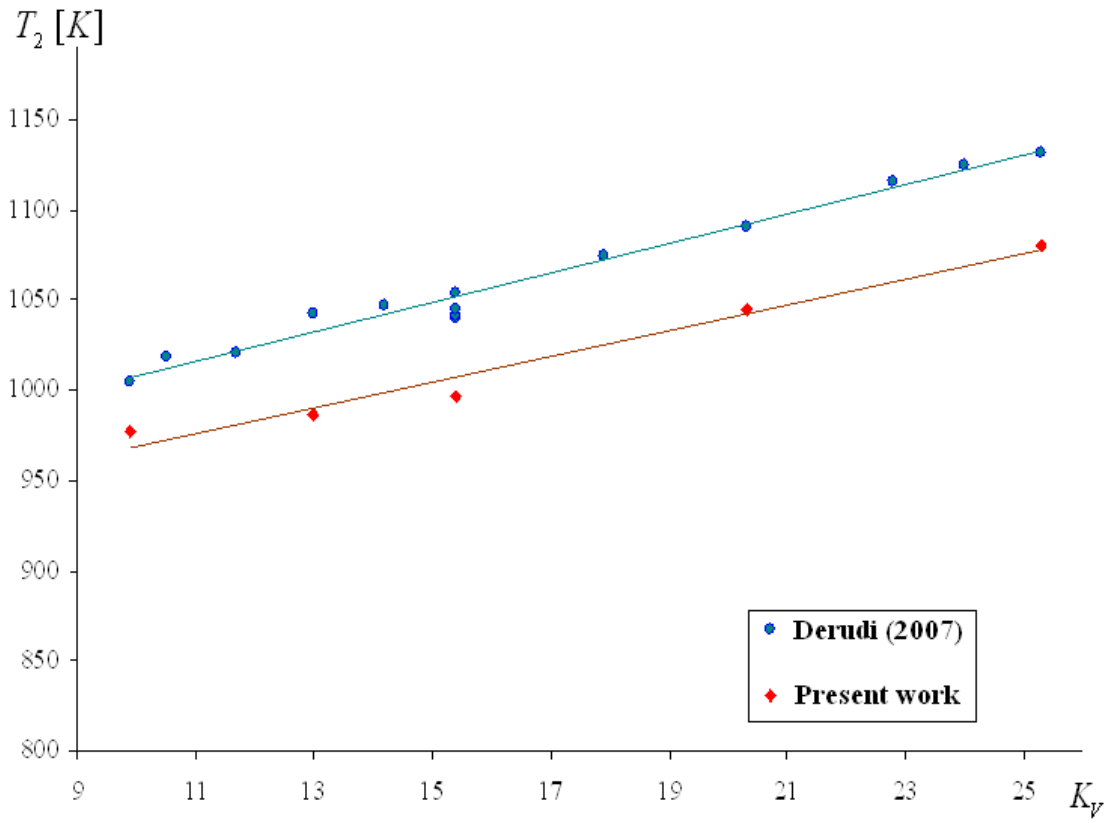

Figure 6: Second probe temperature (z=0.17 m, r=0).

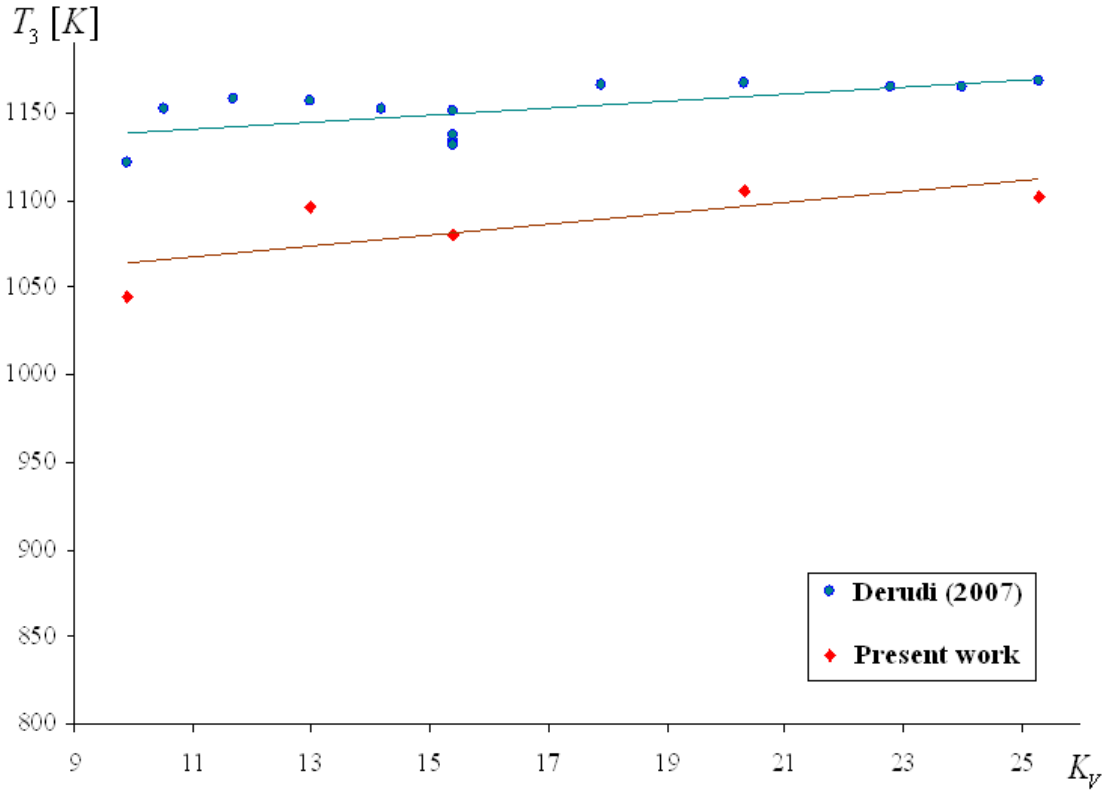

Figure 7: Second probe temperature (z=0.1 m, r=0.01).

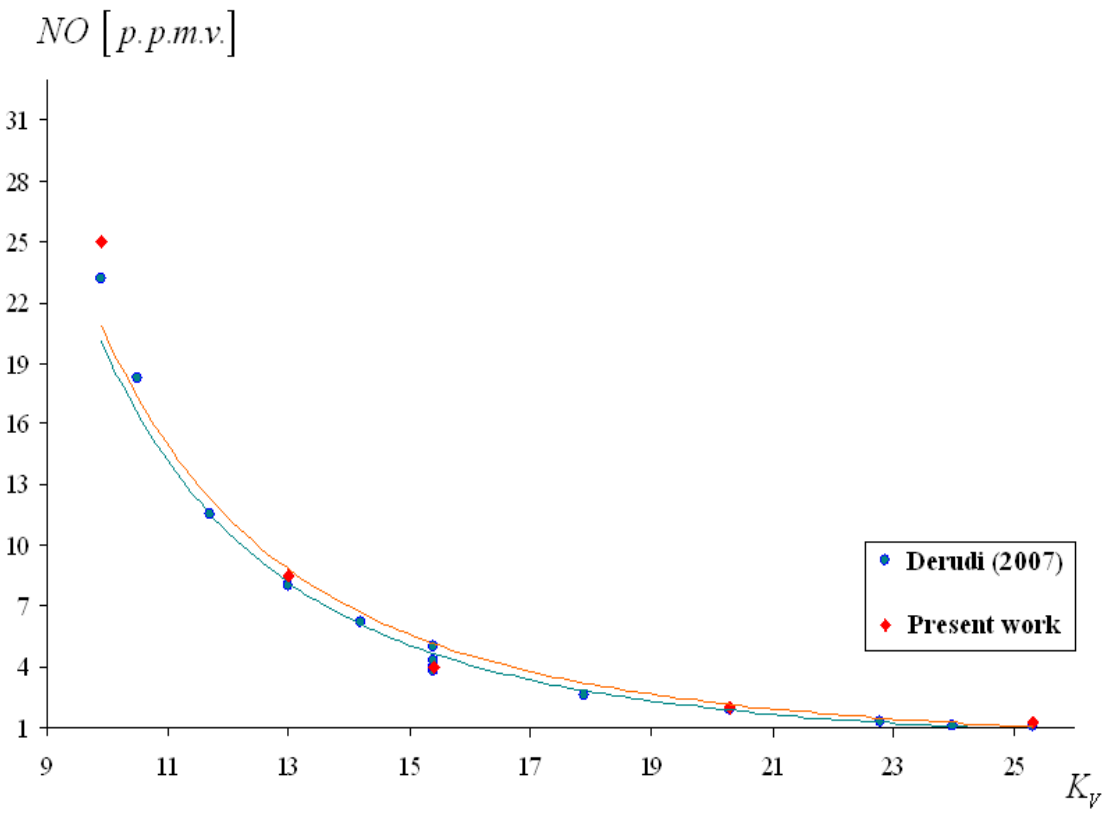

Figure 8: NO emissions [ppmv] at the burner outlet.

3.1 Macroscopic Definition of MILD Regime

In traditional processes a well defined flame front, which involves sharp gradients of temperature and reactants concentration, is observed. In MILD combustion regime, instead, a volumetric combustion takes place. Such a combustion mode, since it is primarily based on strong dilution levels, can be stably sustained only whenever the reactants are above the self–ignition temperature [1].

If this condition is satisfied then the combustion process results intrinsically stable and does not admit the possibility to switch between to two different combustion states [15]. Ignition and extinction phenomena no longer exist and a monotonic shift unburned to burned condition occurs [7,12,16].

It was shown experimentally that, for the hydrogen/oxygen system, in the intermediate temperature range (850-1200 K) a competition between the two main chemical kinetic paths reported in tab. 4 takes place [21,24,25,26]. The second kinetic path prevails in high diluted mixture condition since the oxygen concentration in the first chain branching reaction is reduced and the efficiency of third body in this path is strongly increased (because of the large amount of burnt gases in the mixture).

Thus in MILD combustion regime the second path dominates and fuel self–ignition is due to the destruction of radical H_2O_2 which leads to the formation of two radicals OH [1,21,26] through

$$\mathrm{H_2O_2} + \mathrm{M} \rightarrow \mathrm{OH} + \mathrm{OH} + \mathrm{M} \tag{12}$$

Therefore the characteristic time of reaction (12) may be assumed as the representative time for chemistry in hydrogen MILD combustion:

$$\tau_{\mathrm{chem}} \approx \frac{\rho \cdot Y_{\mathrm{H_2O_2}}}{\dot{\omega}_{\mathrm{H_2O_2}}} \tag{13}$$

Calculating the local fluid dynamic time by

$$\tau_{\mathrm{fluid}} \approx \frac{V_{\mathrm{C}}^{1/3}}{u} \tag{14}$$

where V_c is the computational cell volume, it is possible to define the local Damkohler number as

$$\mathrm{Da} = \frac{\tau_{\mathrm{fluid}}}{\tau_{\mathrm{chem}}} \tag{15}$$

that is always less than unity in the flowfield simulated.

Defining a local stretching time from the strain rate as

$$\tau_{\mathrm{stretch}} \approx \left(\frac{1}{A} \frac{\mathrm{d}A}{\mathrm{d}t} \right)^{-1} \tag{16}$$

the local Karlovitz number can be introduced, *i.e.*,

$$\mathrm{Ka} = \frac{\tau_{\mathrm{chem}}}{\tau_{\mathrm{stretch}}} \tag{17}$$

It is observed that the H_2O_2 Karlovitz number is sufficiently high in the combustion process considered (Ka ≅ 40-200).

Another non–dimensional number which can be introduced in such a process is given by the Kovasznay number, defined as

$$\mathrm{Kz} = \frac{\tau_{\mathrm{chem}}}{\tau_{\mathrm{aero}}} \tag{18}$$

where the local aerodynamic time is given by

$$\tau_{\mathrm{aero}} \approx \sqrt{\frac{15\nu}{\varepsilon}} \tag{19}$$

For all the simulations the asymptotic condition Kz→∞ is practically satisfied (since we have that Kz ≅ 10^5-10^6) so that initial deflagration centres are locally diluted and distributed.

It can be noted that in MILD combustion regime it is no longer possible to define a flame speed and a flame thickness, since no flame front is recognizable. Anyway chemical velocity and length scales can be introduced as those relative to the preheating region, where heat transfer between recirculating burnt products and fresh incoming mixture occurs. Thereby, in order to understand where hydrogen MILD combustion is located on Borghi's diagram [27], the time interval needed by the mixture entering into the preheating region to ignite can be assumed as characteristic chemical time.

Imposing mass conservation in the preheating region one obtains the following velocity:

$$u(r) = u_0 \frac{\rho_0}{\rho(r)} \approx u_0 \frac{p_0}{p(r)} \cdot \frac{T(r)}{T_0} \tag{20}$$

where r is the radial coordinate.

For the burning region it is also possible to write

$$u_b \approx u_0 \frac{\rho_0}{\rho_{\mathrm{b}}} \approx u_0 \frac{p_0}{p_{\mathrm{b}}} \cdot \frac{T_b}{T_0} \tag{21}$$

It is now possible to define a characteristic delay time by the relation

$$\begin{aligned} \tau_{\mathrm{ign}} &= \int_0^{\delta} \frac{1}{u(r)} \mathrm{d}r = \frac{1}{u_0} \int_0^{\delta} \frac{p(r)}{p_0} \frac{T_0}{T(r)} \mathrm{d}r \approx \\ &\approx \frac{1}{u_0} \frac{p_{\mathrm{b}}}{p_0} \int_0^{\delta} \frac{T_0}{T(r)} \mathrm{d}r \end{aligned} \tag{22}$$

Following Semenov's approach [28,29] the energy equation can be written as

$$\rho c_{\mathrm{P}}\, u \frac{\mathrm{d}T}{\mathrm{d}r} = k \frac{\mathrm{d}^2 T}{\mathrm{d}r^2} \tag{23}$$

Integrating eq. (23) with boundary condition $dT/dr=0$ for $r=0$, the temperature gradient is

$$\frac{\mathrm{d}T}{\mathrm{d}r} = \frac{\rho u c_{\mathrm{p}}}{k} \left[T(r) - T_0 \right] \tag{24}$$

Considering this gradient constant within a distance δ (like in Mallard and Le Chatelier's simplified thermal theory [28,29]) one obtains that

$$\frac{\mathrm{d}T}{\mathrm{d}r} \approx \frac{T_{\mathrm{b}} - T_0}{\delta} \tag{25}$$

Therefore it is possible to rewrite eq. (22) as

$$\tau_{\text{ign}} = \frac{T_0}{u_0}\frac{p_{\text{b}}}{p_0}\frac{\delta}{T_{\text{b}}-T_0}\int_0^{\delta}\frac{1}{T(r)}\frac{\mathrm{d}T}{\mathrm{d}r}\mathrm{d}r = \\ = \frac{T_0}{u_0}\frac{p_{\text{b}}}{p_0}\frac{\delta}{T_{\text{b}}-T_0}\ln\left(\frac{T_{\text{b}}}{T_0}\right) \tag{26}$$

Introducing the temperature ratio and density expansion ratio

$$\begin{cases} \vartheta = \dfrac{T_{\text{b}}}{T_0} \\ \gamma = \dfrac{\rho_0 - \rho_{\text{b}}}{\rho_0} \end{cases} \tag{27}$$

the following expression for the characteristic ignition delay time is finally obtained:

$$\tau_{\text{ign}} = \frac{\delta}{u_0}\frac{\ln\vartheta}{\vartheta(1-\gamma)^2} \tag{28}$$

An estimation of δ is given by fig. 12, considering a radial temperature distribution close to the inlet:

$$\delta \approx \frac{T_{\text{inl}}}{(\mathrm{d}T/\mathrm{d}r)_{\text{inl}}} \tag{29}$$

It comes out that $\delta=5\ mm$ and $\tau_{ign}=10^{-2}s$.
Once δ and τ_{ign} have been estimated one can introduce the following

$$u_{\text{b}} \approx \frac{\delta}{\tau_{\text{ign}}} \approx 50\ \text{cm/s} \tag{30}$$

which can be assumed as "characteristic chemical speed".

Assuming the spatial integral scale as the injector diameter $d=3\ mm$ and the velocity fluctuation as

$$u' \approx \sqrt{\frac{2}{3}K} \approx 5\ \text{m/s} \tag{31}$$

it is possible to consider Borghi's diagram [13,30,31] of fig. 13 and to locate the points corresponding to the cases simulated. The single point shown in fig. 13 represents the first case of tab. 1: as expected it is within the volumetric combustion zone on Borghi's diagram.

Now, as far as the Oberlack and Peters' MILD combustion [15] criterion is concerned, condition (1) is checked. For the activation temperature in relation (5) $T_a=8455\ K$, corresponding to

$$\text{O}_2 + \text{H} \rightarrow \text{OH} + \text{O} \tag{32}$$

can be considered: as a matter of fact reaction (32) rules the high temperature pathway, which happens to be disadvantaged in MILD combustion regime [25, 27, 31]. Moreover the second ignition limit is kinetically controlled by the competition between this reaction and $H_2+O_2+M \rightarrow HO_2+M$ [23].

Oberlack and Peters' criterion is fulfilled and results for the cases reported in tab. 1, 2 shown in fig. 14.

Table 4: Hydrogen/Oxygen main competing kinetic paths.

Chain branching path
$O_2 + H \rightarrow OH + O$
$H_2 + O \rightarrow OH + H$
$H_2 + OH \rightarrow H_2O + H$

Chain terminating path
$H + O_2 + M \rightarrow HO_2 + M$
$H_2O_2 + M \rightarrow OH + OH + M$
$H_2 + HO_2 \rightarrow H_2O_2 + H$

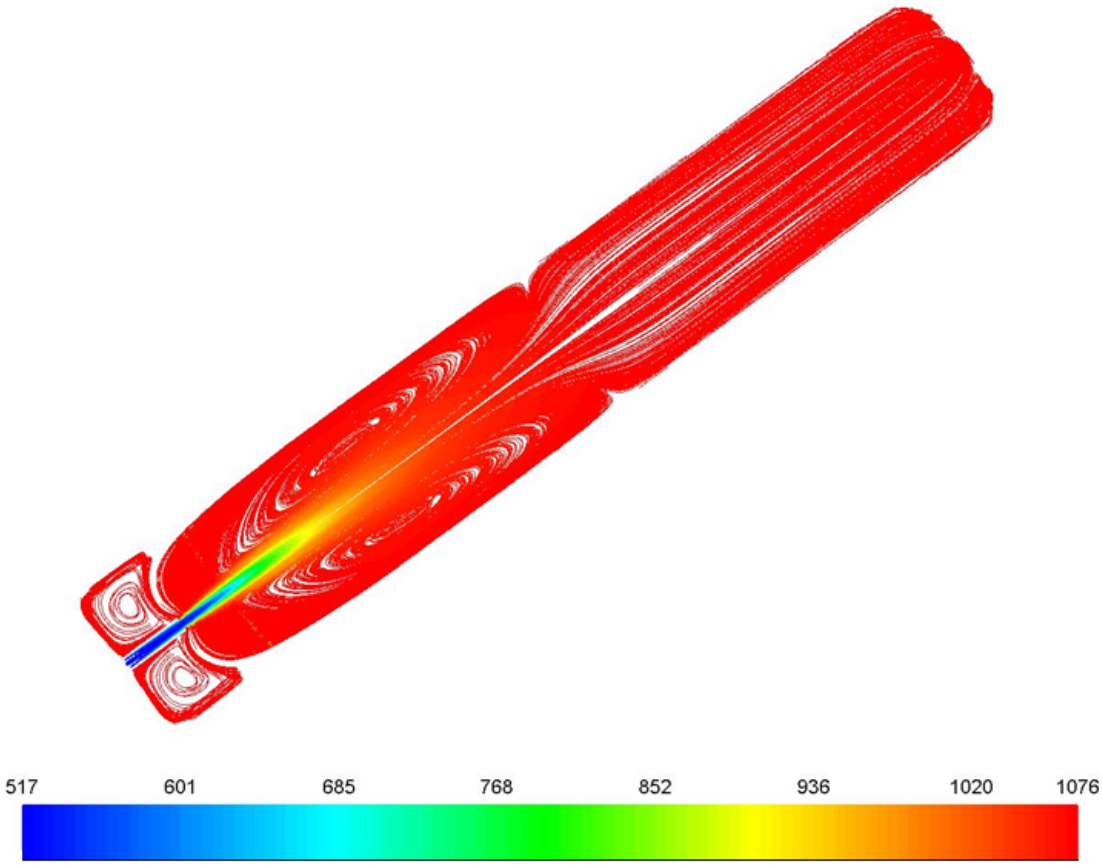

Figure 9: Streamlines coloured by temperature [K].

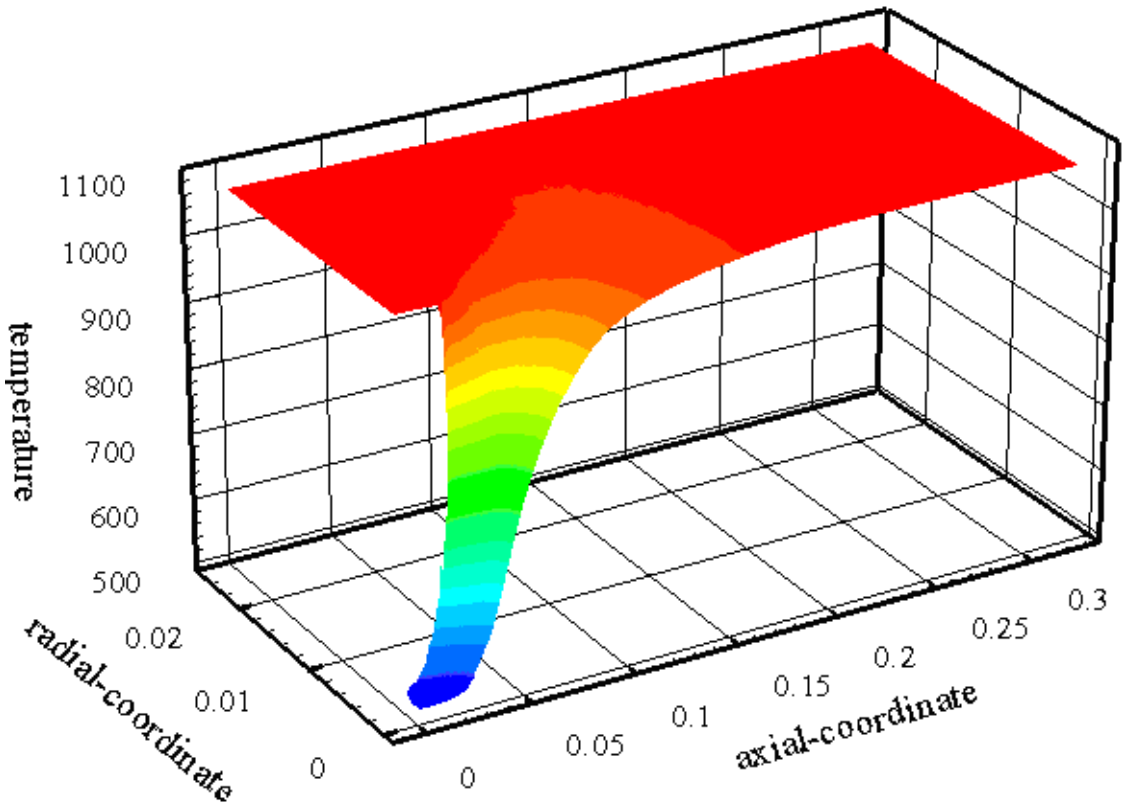

Figure 10: Temperature [K] in the combustion chamber as a function of axial and radial coordinate [m].

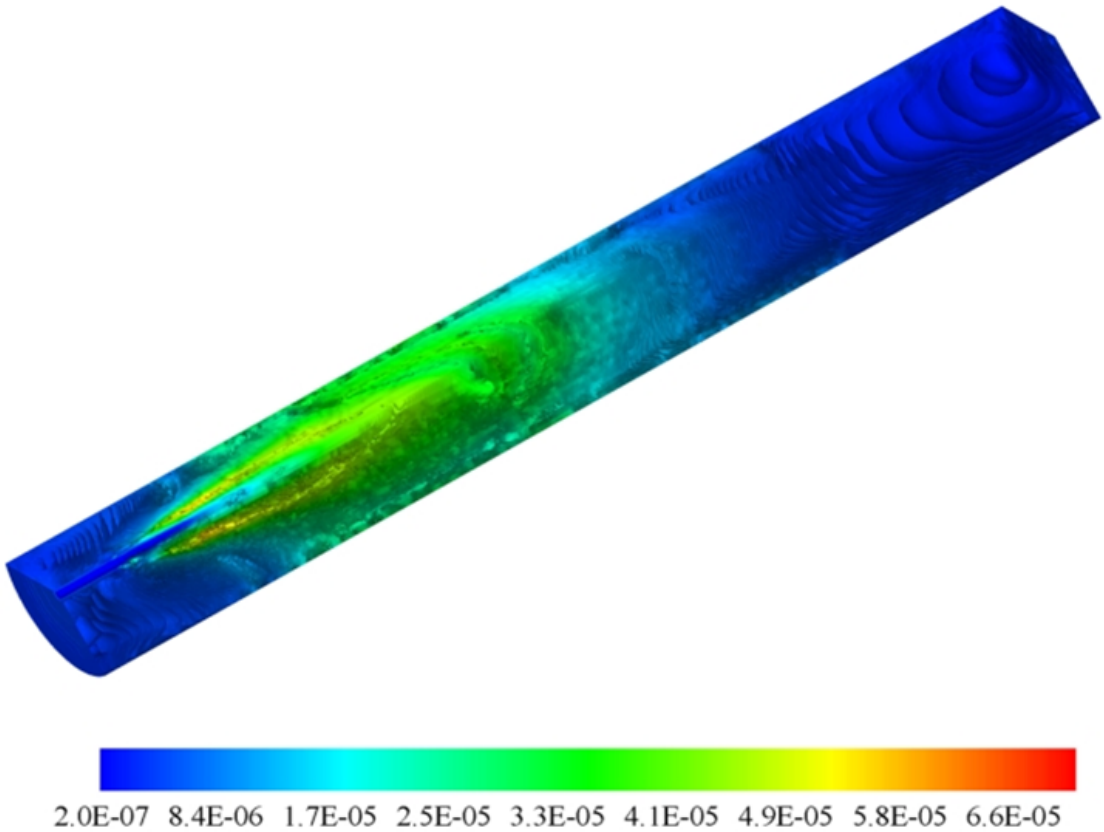

Figure 11: Isosurfaces of OH mass fraction.

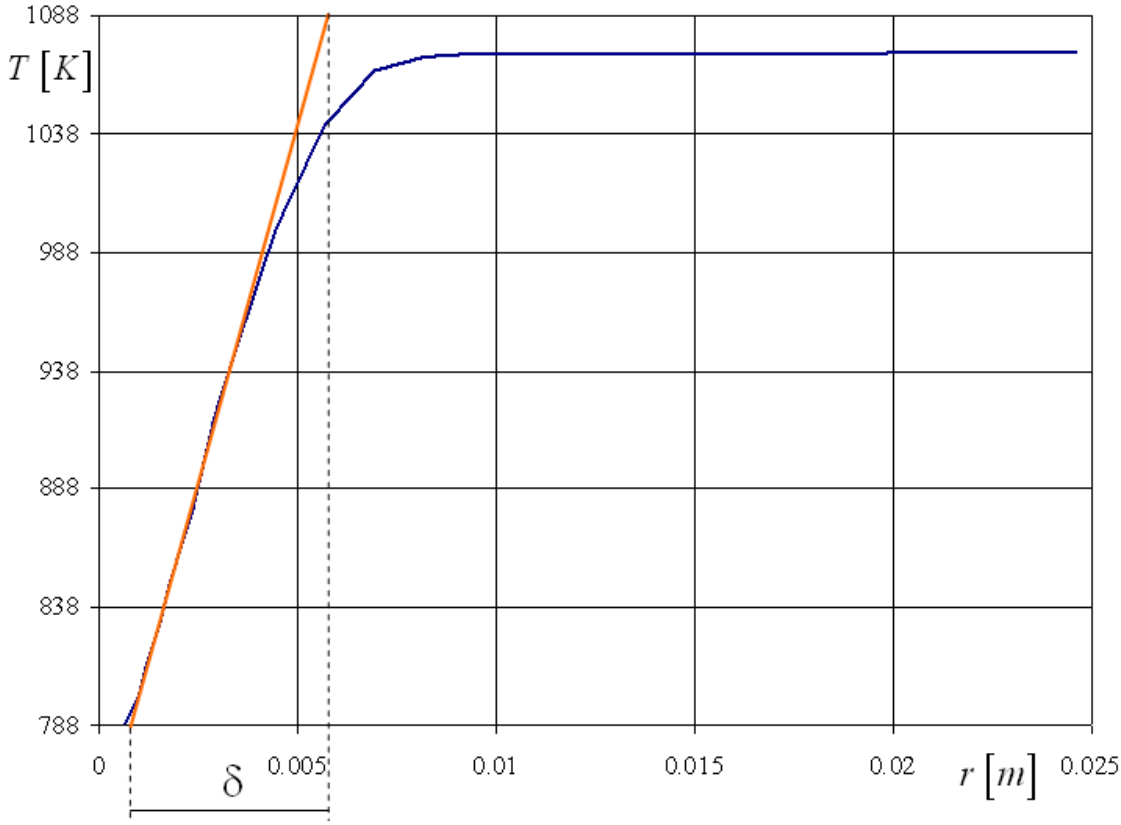

Figure 12: Radial temperature distribution close to the inlet.

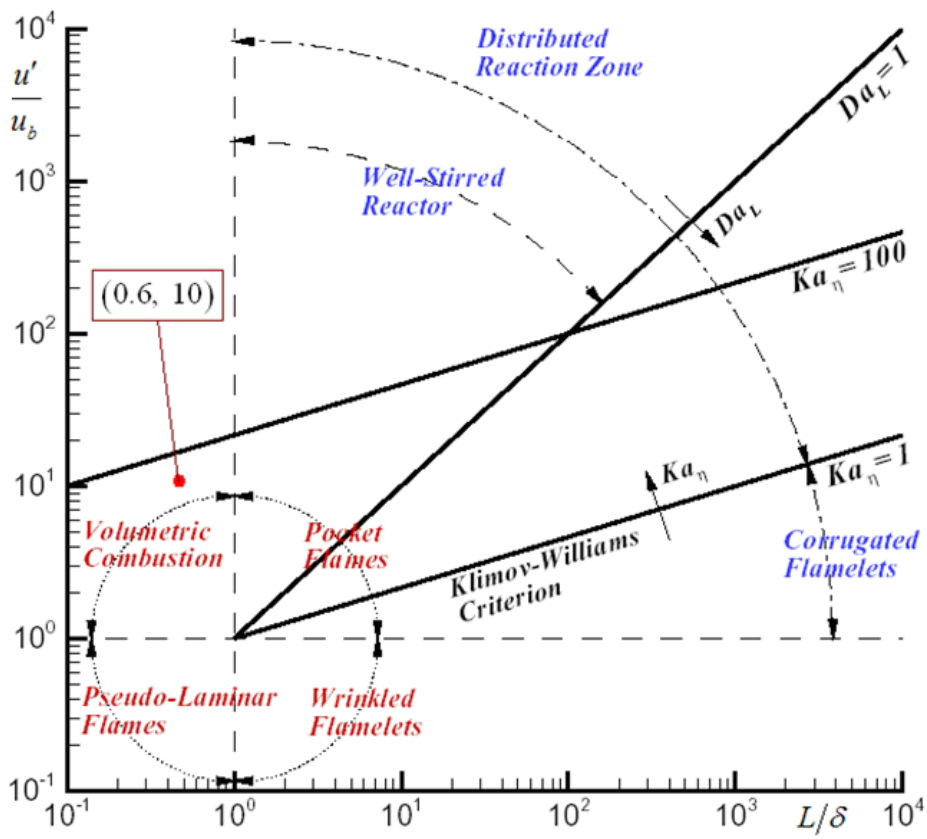

Figure 13: MILD on Borghi's diagram [27] and Klimov-Williams criterion [29] for the first case of tab. 1.

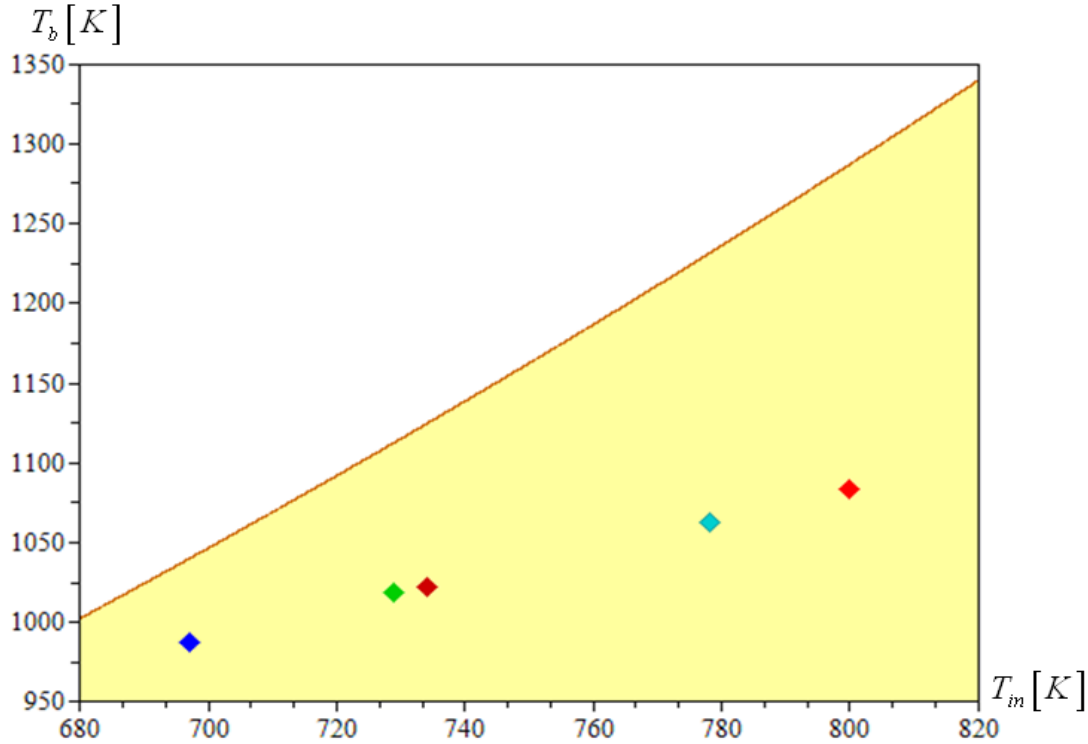

Figure 14: Peters' MILD [15] combustion condition.

3.2 Study of the effect of some parameters

In this section, the effects of recirculation and preheating and the influence of the numerical model are assessed. The main contribution for the establishment of hydrogen MILD combustion seems to be that of incoming mixture preheating: as shown in fig. 15 (which refers to the first case of tab. 1), as long as lower inlet temperatures are used flameless combustion no longer takes place and a flame front is observed (and the system is characterized by higher temperature peaks). Recirculation surely plays an important role but does not happen to contribute as much in the present case: from present results and from further simulations with different recirculation factors it is deduced that the inlet mixture is sufficiently diluted and preheated before entering into the combustion chamber. The further preheating and dilution due to internal recycle are not as essential as they could have been supposed to be.

As far as the numerical model is concerned it is observed that deactivating the radiation model the solution does not vary appreciably. This is due to the fact that the only absorbing/radiating species is H_2O, whose absorption coefficient is small. Hence it may be deduced that in hydrogen MILD combustion radiant energy transfer is not as important as in hydrocarbon MILD combustion.

Besides, the solution seems not to be strongly affected by the chemical kinetic mechanism: no differences were obtained by using Li's [32] mechanism instead of Warnatz's detailed mechanism [23].

Finally, considering adiabatic walls instead of a constant temperature applied on them, it was not observed any difference in the numerical solution. This means that for the apparatus heating of walls is not important when dealing with hydrogen. This observation was also confirmed by personal communications with experimentalists [19] that evidenced the requirement for wall heating in their apparatus when methane is burnt in MILD regime.

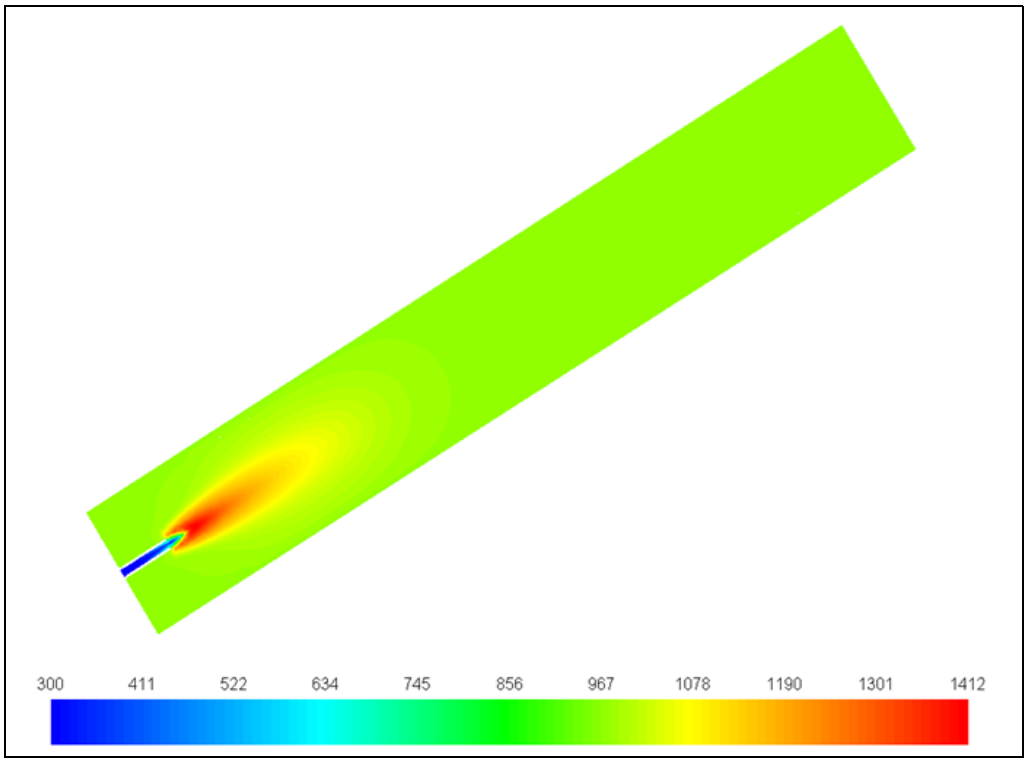

Figure 15: Temperature [K] in a traditional process (first case of tab. 1 with $T_0=300\ K$ at the inlet).

4 CONCLUSIONS

The present paper deals with main chemical and physical aspects of hydrogen MILD combustion. The analysis of such a combustion mode for pure hydrogen as a fuel is led by means of numerical simulations which reproduce Derudi's experimental observations on a small scale apparatus. The results are in good agreement with experimental data and illustrate the main features of flameless combustion, showing a substantial absence of any ignition and extinction phenomena. As a consequence all the reactions are no longer concentrated in the flame front but a volumetric combustion takes place in the burner. High temperature chemical kinetics pathway are in disadvantage with respect to chain terminating reactions: the latter are characterized by local chemical times lower than fluid dynamic times, so that Damkohler number is around one.

Proper definitions for chemical length and velocity scales associated to the preheating region close to the inlet are proposed and by them it is possible to locate MILD regime conditions on Borghi's diagram: the correspondent point falls inside the "volumetric combustion zone".

A nondimensional version of Peters' MILD combustion criterion has been suggested in the case of a hydrogen/air mixture, by considering high temperature main reaction activation energy in the analytical condition. For all the cases simulated such condition is observed to be satisfied.

The effect of preheating and recirculation is finally analyzed carrying out further simulations with different values of such parameters: the main contribute is observed to be due to preheating. Turning off the radiation model, changing the chemical mechanism or separately does not considerably affect the numerical solution of the present test case.

REFERENCES

[1] A. Cavaliere and M. de Joannon, MILD Combustion, *Progress in Energy and Combustion Science*, **30**, pp. 329–66 (2004)

[2] G. Choi and M. Katsuki, Chemical kinetic study on the reduction of nitric oxide in highly preheated air combustion, *Proceedings of the Combustion Institute*, 29, 1, pp. 165–71 (2002)

[3] B. B. Dally, A. N. Karpetis and R. S. Barlow, Structure of turbulent non–premixed jet flames in a diluted hot coflow, *Proceedings of the Combustion Institute*, 29, 1, pp. 147–54 (2002).

[4] A. K. Gupta, S. Bolz, and T. Hasegawa, Effect of Preheat Temperature and Oxygen concentration on Flame Structure and Emission, *Journal of Energy Resources Technology*, **121**, 3, pp. 209–16 (1999).

[5] M. Katsuki and T. Hasegawa, The Science and Technology of Combustion in Highly Preheated Air, *Proceedings of the Combustion Institute*, 27, pp. 3135–46 (1998).

[6] E. Mastorakos, A.M.K.P. Taylor and J.H. Whitelaw, Extinction of Turbulent Counterflow Flames with Reactants Diluted by Hot Products, *Combustion and Flame*, **102**, pp. 101–14 (1995).

[7] N. Peters, Principles and potential of HiCOT combustion, *Proceedings of the Forum on High–Temperature Air Combustion Technology*, Japan, pp. 109–128 (2001).

[8] A. Cavigiolo, M.A. Galbiati, A. Effuggi, D. Gelosa and R. Rota, MILD Combustion in a Laboratory–Scale Apparatus, *Combustion Science and Technology*, **175**, pp. 1347–67 (2003).

[9] B.B. Dally, E. Riesmeier and N. Peters, Effect of fuel mixture on moderate and intense low oxygen dilution combustion, *Combustion and Flame*, **137**, pp. 418–31 (2004).

[10] M. Derudi, A. Villani and R. Rota, Sustainability of MILD Combustion of Hydrogen–containing Hybrid Fuels, *Proceedings of the Combustion Institute*, 31, pp. 3393–400 (2007).

[11] A. Galbiati, A. Cavigiolo, A. Effuggi, D. Gelosa and R. Rota, MILD Combustion for Fuel NO_x Reduction, *Combustion Science and Technology*, 176, pp. 1035–54 (2004).

[12] T. Plessing, N. Peters and J.G. Wunning, Laseroptical Investigation of Highly Preheated Combustion with Strong Exhaust Gas Recirculation, *Proceedings of the Combustion Institute*, 27, 3, pp. 197–204 (1998).

[13] J.A.Wunning and J.G. Wunning, Flameless oxidation to reduce thermal NO formation, *Progress in Energy and Combustion Science*, **23**, pp. 81–94 (1997)

[14] A. Milani, MILD Combustion techniques applied to regenerative firing in industrial furnaces, *Proceeding of 2nd International Seminar on High Temperature Air Combustion in Industrial Furnaces*, Stokholm (2000).

[15] M. Oberlack, R. Arlitt and N. Peters, On stochastic Damkohler number variations in a homogeneous flow reactor, *Combustion Theory and Modeling*, **4**, pp. 495–509 (2000).

[16] I.B. Ozdemir and N. Peters, Characteristic of the reaction zone in a combustor operating at MILD combustion, *Experiments in Fluids*, **30**, pp. 683–95 (2001)

[17] C. Galletti, A. Parente, L. Tognotti, M. Derudi, A. Villani and R. Rota, Experimental and Numerical Investigation of a Burner Operating in MILD Combustion Conditions, *3rd Europeran Combustion Meeting* (2007).

[18] P. Spalart and S. Allmaras, A one–equation turbulence model for aerodynamic flows, *AIAA–92–0439* (1992).

[19] M. Derudi, Personal communication (2008).

[20] A.P. Morse, Axisymmetric Turbulent Shear Flows with and without swirl, *Ph. D. thesis*, London University, UK (1977).

[21] B.F. Magnussen, On the Structure of Turbulence and a Generalized Eddy Dissipation Concept for Chemical Reaction in Turbulent Flow, *19th AIAA Meeting, St. Louis* (1981).

[22] P. Cheng, Two–Dimensional Radiating Gas Flow by a Moment Method, *AIAA Journal*, **2**, pp. 1662–4 (1964).

[23] U. Maas and J. Warnatz, Ignition Processes in Hydrogen–Oxygen Mixtures, *Combustion and Flame*, **74**, pp. 53–69 (1988).

[24] Y.B. Zeldovich, The oxidation of Nitrogen in combustion and explosions, *Acta Physiochimica* XXI, U.R.S.S. (1946).

[25] F. Behrendt and J. Warnatz, The dependence of flame propagation in H_2–O_2–N_2 mixtures on temperature, pressure and initial composition, *International Journal of Hydrogen Energy*, **10**, 11, pp. 749–55 (1985).

[26] J.A. Miller and C.T. Bowman, Mechanism and Modelling of Nitrogen Chemistry in Combustion, *Progress in Energy and Combustion Science*, **15**, pp. 287–338 (1989).

[27] R. Borghi, Turbulent combustion modelling, *Progress in Energy and Combustion Science*, **14**, pp. 245–92 (1988).

[28] I. Glassman, Combustion, *Academic Press*, San Diego, (1996).

[29] N. Peters, Turbulent Combustion, *Cambridge University Press*, Cambridge (2000).

[30] J. Strohle and T. Myhrvold, An evaluation of detailed reaction mechanisms for hydrogen combustion under gas turbine conditions, *International Journal of Hydrogen Energy*, **32**, pp. 125–35 (2007).

[31] C.K. Westbrook, Chemical kinetics of hydrocarbon ignition in practical combustion systems, *Proceedings of the Combustion Institute*, 28, pp. 1563–77 (2000).

[32] J. Li, Z. Zhao, A. Kazakov and F.L. Dryer, An Updated Comprehensive Kinetic Model of Hydrogen Combustion, *International Journal of Chemical Kinetics*, **36**, pp. 566–75 (2004).